Contemporary Mathematics
Volume **693**, 2017
http://dx.doi.org/10.1090/conm/693/13952

Tracking the structural deformation of a sheared biopolymer network

Louise M. Jawerth and David A. Weitz

This paper is dedicated to Björn Jawerth

Abstract. Biopolymer networks provide mechanical integrity in many important environments *in vivo* ranging from the cytoskeleton within a cell to the structural support of cells themselves in tissues and tendons. Rheological studies have shown that they exhibit many unique material properties. Modelling these properties requires a precise knowledge of how the individual filaments in the network deform locally during a global deformation. Here, we present an image processing method to track the three-dimensional motion of a biopolymer network as a simple shear deformation is applied. We track the structure of the network from one shear position to the next by determining the displacement of each branch point using a cross-correlation. To illustrate the use of this algorithm, we apply it to a fluorescently labelled fibrin network.

Introduction

Biopolymer networks provide mechanical integrity in many important environments *in vivo* ranging from the cytoskeleton within a cell to the structural support of cells themselves in tissues and tendons. These networks are composed of protein sub-units that polymerize into long fibers which self-associate to form the network itself. To understand their behavior in the complex environment of a living organism, the material properties of biopolymers are routinely studied in the absence of other proteins *in vitro*. Rheological studies characterizing the force required to deform a biopolymer network have shown that they exhibit many unique material properties, such as strain stiffening([**SPM05**] [**BM14**]). For many of these measurements, the networks are subjected to a simple shear strain: the network is held between two parallel plates and the top plate is translated while the bottom plate remains fixed. Modelling the material properties of biopolymer networks requires a precise knowledge of how the individual filaments in the network deform locally during such a global deformation ([**BM14**]); however, there currently exist no experimental methods that quantitatively track the motion of individual fibers as a network is deformed. Such a method is essential to directly test the validity of current models and for the development of new ones.

Confocal fluorescence microscopy is a powerful technique to resolve the three-dimensional structure of many biopolymer networks ([**JMV10**]). Networks in

2010 *Mathematics Subject Classification.* Primary 92C05, 74-04, 68U10.
Key words and phrases. Image processing, fibrin, shear.

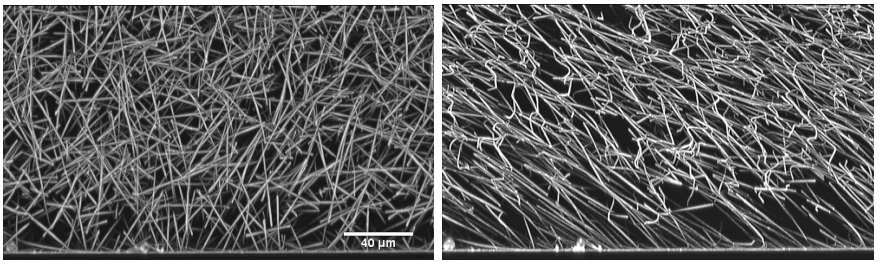

(A) (B)

FIGURE 1. A) A fluorescently labelled fibrin network before any deformation is applied. B) The same region with an applied shear strain.

which the average spacing between fibers is larger than a micron, such as those found in bundled actin systems, collagen and fibrin are particularly amenable to this technique ([**BKC08**] [**MJL13**], [**JMV10**]). Typically for this technique, some of the protein sub-units are tagged with fluorophores that emit light when excited. The acquired images are gray-scale with pixel values corresponding to the emitted light intensities; thus, fibers appear as bright filaments on a dark background. To image a three-dimensional region, a series of images is taken at increasing z positions where each image represents a cross-section of the network in xy; each such series of images is referred to as an image stack. Such a procedure can be repeated to capture the behavior of a network over time or in response to a deformation ([**MJL13**]). Previous studies have developed methods to extract the position of fibers taken in a single image stack. Typically, they result in a one-pixel thick line that follows along the axis of each fiber in the network. Amongst other terms, the positions of the fibers along their axes is referred to alternatively as the skeleton, medial axis, backbone or centerline ([**KML12**] [**SVJ08**] [**MMJ**] [**XVH**]). In this paper, we refer to the results of such a method as the skeleton of the network. Yet, despite the ability to quantitatively identify the structure of a biopolymer network, no image processing methods exist to quantitatively track how the structure of a network changes from one image stack to another. Such a method is imperative to extract how the individual fibers in a network deform when sheared. From this we could discern the physical principles underlying the unique properties exhibited by biopolymer networks *in vitro*, thus broadening our understanding of their behavior in the more complex environment of a living organism.

Here, we present an image processing method to track the three-dimensional motion of a biopolymer network as it is sheared. The data is assumed to be in the form of image stacks that are taken at several time points as the network is increasingly sheared (see Fig. 1).We first extract the three-dimensional skeleton of the biopolymer network using existing techniques and subsequently apply our method. We find that network branch points represent unique features and utilize this to track the structure of the network from one shear position to the next. We demonstrate this method for a fluorescently labelled fibrin network.

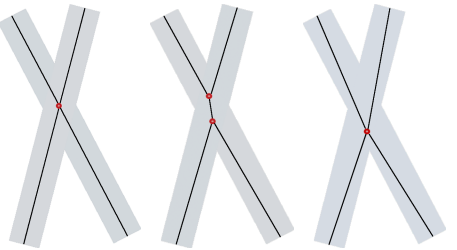

FIGURE 2. An illustration of typical variations that occur during skeletonization. Intersecting fibers are shown in light gray, the identified branch points are shown as red dots and the skeleton is indicated as a black line. A) One possible skeletonization where one branch point is identified. B) A second example illustrating how two branch points can easily be identified instead of one. C) A skeletonization where the branch point is located at a slightly different position as compared to the branch point in A.

THE METHOD

Overview of the Tracking Algorithm

One approach to tracking a network would be to identify the skeleton of the network at every time point and then determine how one skeleton must deform to assume the position and shape of the subsequent one. In practice, such a method is difficult to implement because the results of a skeletonization algorithm are subject to some variations when performed on two datasets. For instance, a node representing the junction of four fibers may sometimes be skeletonized properly as the junction of four fibers, but is also likely to be skeletonized into two T-junctions connected by a small fiber (see Fig. 2B). Similarly, the exact location of a node may change slightly each time the data is skeletonized (see Fig. 2C). These types of artifacts make the process of finding the proper correspondence between a network skeletonized at two different time points very difficult. Instead of using such an approach, we utilize the fact that under most circumstances associated fibers remain bound, do not break and do not associate with new fibers as a network is deformed ([**MJL13**]). This entails that the network topology remains fixed. Therefore, our algorithm is not concerned with extracting the three-dimensional network structure; rather, once a structure has been identified, this algorithm determines how the structure deforms over time. We achieve this by skeletonizing the network in the first time point. After which, we find the displacement of the network to each subsequent time point using a method based on cross-correlations of the gray-scale values of three-dimensional regions centered around feature points. We track nodes that are the junctions between three or more fibers during the deformation; physically, these nodes represent branch points in the network.

Our approach can be summarized as follows (see Fig. 3). We identify the initial three-dimensional skeleton of the network and all its node positions. We denote each node by its linear index, i. The gray-scale voxel region around each node at the initial time point represents the feature to be tracked (denoted, f_i). For

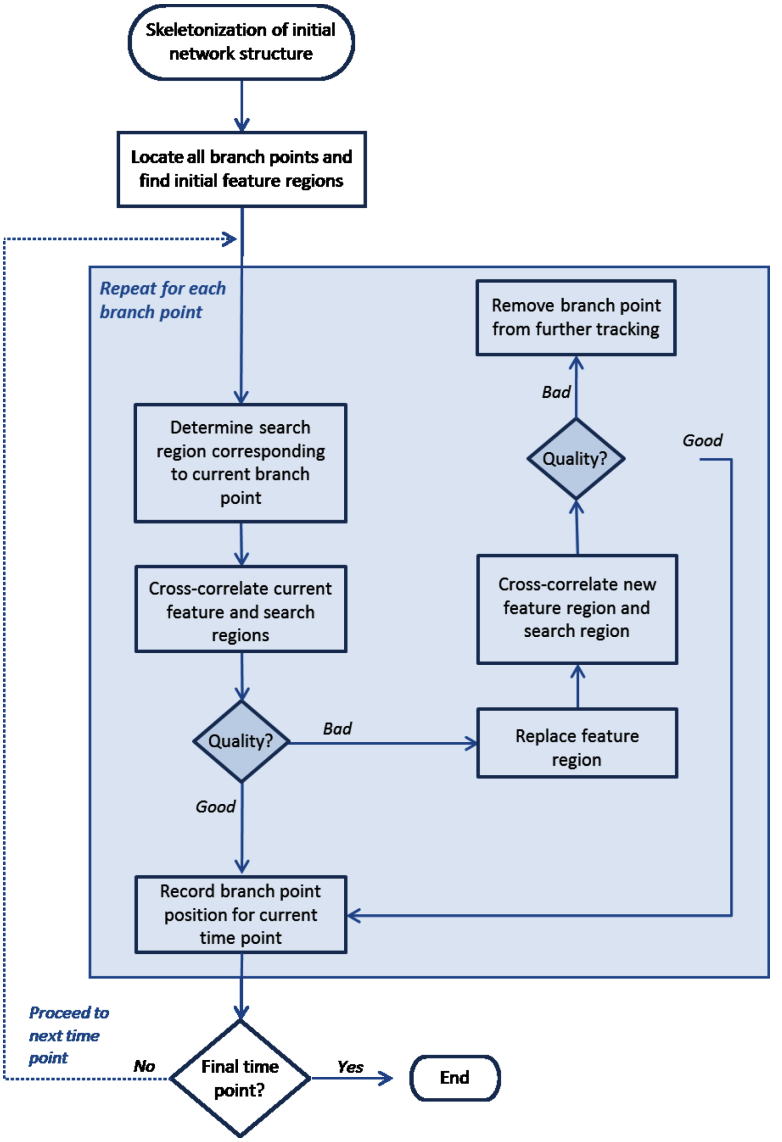

FIGURE 3. Algorithm flow chart

each time point t and node i, we select a voxel search region where we expect the node to be located, $s_i(t)$. We cross-correlate f_i with the search region, $s_i(t)$. The location at which the value of the cross-correlation (CC) is maximal, represents the three-dimensional displacement of the feature from the one frame to the next. The CC is deemed successful if one or more quality measures exceed a threshold level. If the CC is successful, we record the corresponding displacement as the position of the node at that time point.

If the CC fails, we replace f_i with a voxel region taken from the previous time point, $t - 1$, in which the node was successfully located. We cross-correlate this updated feature region with the search region. If the CC again fails, the feature is

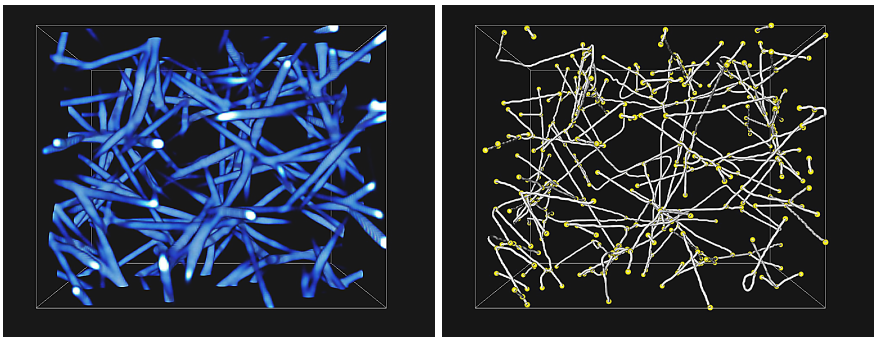

(A) (B)

FIGURE 4. A) The original image rendered to show the three-dimensional structure of a small region in a typical network B) The corresponding area with the skeleton represented by gray tubes and the branch points marked with small yellow spheres.

considered "lost" and will not be tracked through further timepoints. If this CC is, instead, successful, we record the node position at this time point and continue with this new feature region for further time points. We repeat this procedure for all nodes, i in the network and then proceed to the next time point.

In the next sections we review the details of this procedure.

1. Initial Processing: Network Extraction

There are many algorithms that can be used to find the skeleton of a network (for a good overview of such methods please see [**XVH**]). To use the algorithm described here it is important that the branch points or intersections between fibers are identified as part of the algorithm (see Fig. 4).

2. Selection of features and search regions

2.1. Selection of initial feature regions. Typically, a network is composed of fibers that are relatively uniform in intensity and width. A small section of one fiber is generally indistinguishable from another one (see Fig. 6). It is therefore difficult to track fiber segments. By contrast, the points where fibers branch are excellent features to track: Each such node is the junction between several fibers with relative angles that are distinct when compared to those of other nodes (see Fig. 5 and Fig. 6). Moreover, these characteristics do not change significantly for small network deformations. From the initial network extraction, we know the locations of all the nodes in the network in the first time point. We use a small voxel region of the gray-scale image stack taken from this time point centered about each node, i, as the feature, f_i, that will be tracked. We found that a voxel region large enough to enclose the node and the fibers but small enough to avoid most of the length of the fibers was ideal (see Fig. 5A).

2.1.1. *Replacement of feature regions.* As a fibrin network is deformed, we found that the fibers that join at some nodes will gradually rotate or buckle from one time point to the next. This can lead to a persistent deformation that, once great enough, the node may no longer closely resemble itself at the initial time

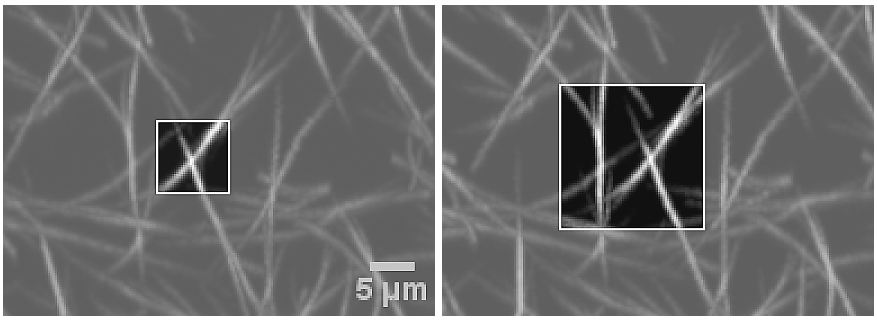

(A) Feature Region (B) Search Region

FIGURE 5. Maximum projections of a region taken from a deforming fibrin network. A) The feature region is outlined in white (size: $32x32$ pixels) B) The corresponding search region taken at the following time point outlined in white (size: $64x64$ pixels).

point. In our algorithm, the node displacement is given by matching the feature region within a search region. If the node is too deformed in the search region as compared to the feature region, it no longer becomes possible to find a match. When this occurs, we replace the current feature region with a similarly sized region taken from the last time point in which the node was successfully located. With this procedure, as long as the deformation of a node is small between time points, the node position can still be successfully tracked.

2.2. Selection of a search region. A search region is a region in the network where we expect a specific node to be located. In our initial approach, we chose a search region centered around the node position in the previous time point; however, we found that in a sheared network, nodes located closer to the translated upper plate move significantly more than those close to the stationary bottom surface. In fact, this motion can be so large that the node has moved out of the neighborhood of its previous location. We therefore found that in practice it is more accurate to choose a search region centered about the predicted position of a node. Since we are applying a shear to the network, we assume that the predominate deformation of the network is that of an affine, shear deformation. This implies that for a node with a position x, y, z, its predicted position x_p, y_p, z_p is given by,

$$\begin{bmatrix} x_p \\ y_p \\ z_p \end{bmatrix} = \begin{bmatrix} 1 & 0 & 0 \\ 0 & 1 & \gamma \\ 0 & 0 & 1 \end{bmatrix} \begin{bmatrix} x \\ y \\ z \end{bmatrix} \tag{2.1}$$

where γ is the amount of shear imposed in the experiment; this value is defined as $\gamma \equiv -d/h$ where d is the displacement of the top glass plate during one shear step and h is the height between the top and bottom plates (see Fig. 6 and Fig. 7). In our datasets, we sheared in the $-y$ direction and γ is negative. However, the deformation tensor can easily be modified for any shear direction.

For every node, i, we calculate its expected position and define a voxel region, $s_i(t)$, centered at that expected position from the image stack representing the time point, t. Generally, we found that a region larger than the feature region was needed to accurately locate a node during our tracking (see Fig. 5).

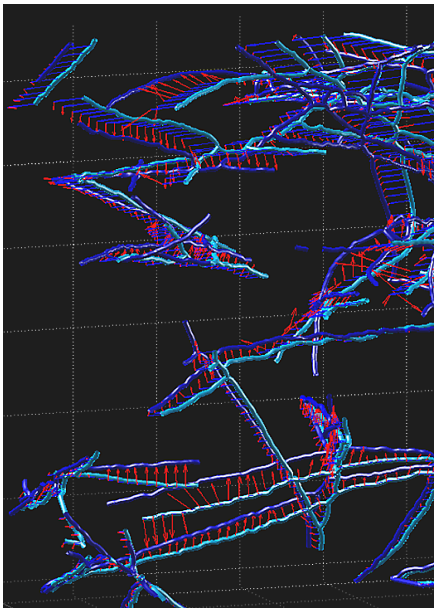

(A)

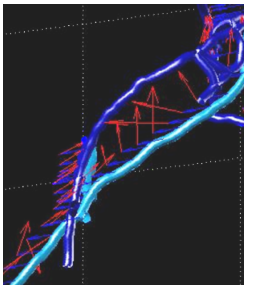

(B)

FIGURE 6. A) The light blue structure is the initial skeleton and the dark blue structure is a skeleton found at a later time point. For this image, we have tracked the structure using CCs as described in this paper with the modification that all possible feature points along the fibers were cross-correlated, not just the branch points of the network. The blue arrows indicate the expected fiber positions based on a simple shear deformation. The red arrows mark the deviation from the expected position and the displacement found from the cross-correlation. B) An example of the errors that occur when fiber segments are cross-correlated. The red arrows show that a fiber segment is being matched with an incorrect segment in the later time point.

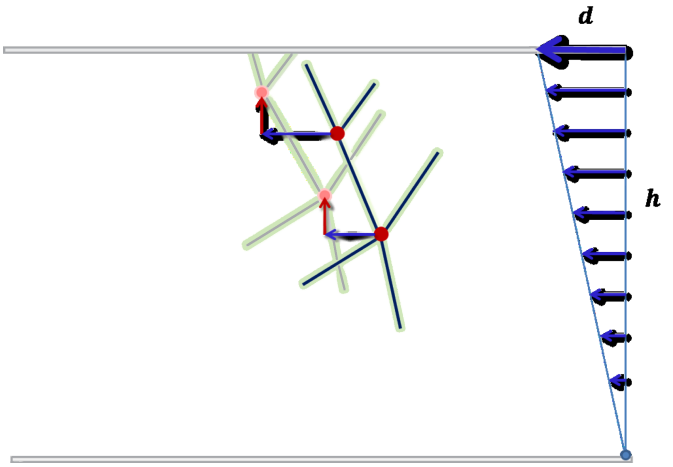

FIGURE 7. An illustration of two branch points in a network. The initial branch point positions are shown in bold colors and the branch point positions in the next time point are shown in lighter colors. The shear, γ, on the network is given by $\gamma = -d/h$, where d is the distance the top plate has moved and h is the distance between the two plates. The farther a branch point is away from the bottom plate, the more it is expected to move; this is illustrated by the shear profile shown with blue arrows on the right. For the two branch points illustrated in this diagram, their expected motion is shown with blue arrows, and the correction from this expected motion to their actual displacement is shown with red arrows.

3. Finding the displacement of a feature region within the corresponding search region

In this section we describe how the position of one node, i, is located at a time, t. Since we are just treating one node and one time point, for a cleaner notation we have neglected to write the index i and specify the time t. Specifically, in this section we will refer to s_i and f_i as s and f, respectively. All search regions are taken from the current time point, t, and all feature regions are taken either from the initial time point or from their most recently updated time point (see section 2.1.1) Moreover, for a feature region, we refer to $f(x, y, z)$ to denote the value of f for the voxel located at the point (x, y, z) within this region. Voxels within s and our cross-correlation C are denoted similarly.

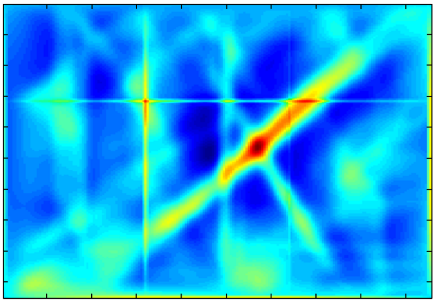

FIGURE 8. One XY plane through C for the cross-correlation between the feature region and search region shown in Fig. 5

3.1. Cross-correlation method to find one node displacement. To locate the node position, we calculate the cross-correlation $C(x, y, z)$ between $s(x, y, z)$ and $f(x, y, z)$. The cross-correlation is defined as

$$C(x,y,z) = \frac{\sum_{u,v,w}(f(u+x,v+y,w+z)-\overline{f}(x,y,z))(s(u,v,w)-\overline{s}(x,y,z))}{\sqrt{\sum_{u,v,w}(f(u+x,v+y,w+z)-\overline{f}(x,y,z))^2}\sqrt{\sum_{u,v,w}(s(u,v,w)-\overline{s}(x,y,z))^2}} \tag{3.1}$$

where $\overline{f}$ is the mean of f and $\overline{s}$ is the mean of s each in a box the size of f centered at (x, y, z).The denominator corresponds to the auto-correlation of each function. It normalizes the function so that if the two functions correlate perfectly the result is 1 and -1 if they are perfectly anti-correlated.

The position (x, y, z) with the maximum value of C corresponds to the relative shift between the centers of f and s (see Fig. 8). Briefly, this approach moves a normalized feature region around in a normalized search region. For every translated position (x, y, z), the product of each voxel in the normalized feature region with the corresponding underlying voxel in the normalized search region is calculated; this product is the value $C(x, y, z)$. The position with the greatest value (the maximum of C) corresponds to the translated position with the best match.

3.1.1. *Quality Measures.* There are two measures we used to examine the quality of the cross-correlation. The first is the magnitude of the cross-correlation at its maximum. For a normalized cross-correlation, as in equation 3.1, a value of 1 corresponds to a perfect match and a value of -1 corresponds to a perfect mismatch. A threshold value can be set as a quality measure for the cross-correlation. However, we found that in practice a different quality measure was often more accurate in identifying a poorly matched point: When a node did not cross-correlate well its displacement was very large. This was due to the dark areas around the fibers matching well; therefore, a good second quality measure was to only allow displacements smaller than a threshold displacement. In summary, a cross-correlation is considered successful if the maximum of C is larger than a threshold value and/or the displacement is smaller than a threshold displacement; otherwise the cross-correlation is considered failed.

Application of algorithm to a fibrin network undergoing shear

4. Details of data acquisition and application of the tracking algorithm

To illustrate the use of this algorithm, we apply it to a fibrin network as it is sheared. We polymerize a fluorescently labelled fibrin network between two glass plates on a confocal microscope (Leica SP5, 63x 1.2NA equipped with a water immersion objective). Once polymerization is complete, we acquire a stack of images representing a three-dimensional region of the network (approximately $250\mu mx250\mu mx100\mu m$) (see Fig. 1). By translating the upper-glass plate parallel to the bottom plate, we impose a simple shear deformation on the fibrin network. We translate the upper-glass plate in increments corresponding to approximately 1% shear steps. After each movement, we acquire a new stack of images corresponding to the increasingly deformed fibrin network.

To track the deformation of the network, we use the following parameters.

(1) *Pre-processing:* We smoothed the image stack corresponding to the first time point using a Gaussian filter to suppress acquisition noise. Subsequently, we determined the skeleton using the commercial software package AMIRA (FEI Software, Ver 5.3).
(2) *Size of feature region:* $32x32x32$ voxels (see Fig: 5A)
(3) *Size of search region:* $64x64x64$ voxels (see Fig: 5B)
(4) *Cross-correlation quality measure:* For displacements larger than 8 voxels, we considered a cross-correlation unsuccessful.

We track the branch points in the network for 50 time points. We take a maximum projection of one small region and overlay this with the tracked positions in this region (see Fig. 5). We carefully inspect the accuracy of the algorithm. We find that many of the branch points are accurately located from one time point to the next. When a branch point is unsuccessfully tracked it is often the result of an aberrant branch point found in the initial skeletonization. These branch points occur when two fibers cross close to each other without adhering to one another. During skeletonization, this can appear to be the junction or branch point between four fibers.

5. Discussion

In this paper, we have presented an image processing method that tracks the structure of a biopolymer network as it is sheared. As an initial step, we have taken the skeleton of a network using an existing skeletonization technique. In general, however, our algorithm does not require the existence of a network skeleton. Since the algorithm cross-correlates regions from the original gray scale image stacks, it just requires knowledge of the position of network branch points. We, however, did not know of other algorithms that identify fiber branch points and therefore relied on skeletonization routines. Using a skeleton in the initial time step is also advantageous because it determines how individual branch points are connected. Together with the motion of the network, the connectivity of a branch point has been an important consideration in many models of network mechanics ([**BMLM11**] [**LMS15**]). Moreover, since branch points are connected via a fiber,

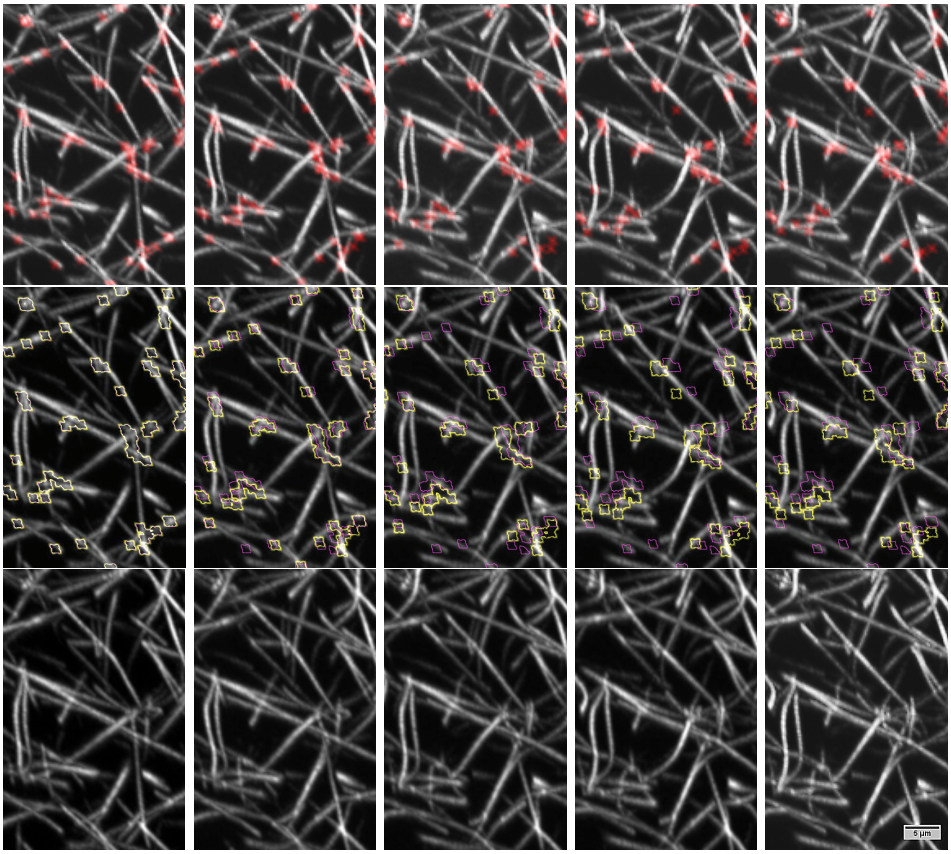

$\gamma = 0\%$ $\gamma = 5\%$ $\gamma = 10\%$ $\gamma = 15\%$ $\gamma = 20\%$

FIGURE 9. A small region of a fibrin network with different amounts of shear strain applied. For clarity, in these images, we have transformed the sheared images using a simple shear deformation (see the Materials and Methods section). The motion of the network that remains is movement around the expected shear deformation. The branch points are indicated in red in the upper panels. These same points are outlined in the middle panels in yellow with the magenta outlines indicating the original undeformed branch point positions. The lower panels are the same region without the branch points outlined The z-direction corresponds to the vertical direction in these images.

by measuring the relative displacement between the two fiber ends, one can calculate values such as the elongational strain across individual fibers. This is also an important parameter in many models of network mechanics ([**SPM05**][**MKJ95**]).

Our algorithm is based on using cross-correlations to track the positions of branch points in a network. We perform the cross-correlations on the original gray-scale images. The exact location of a branch point may vary slightly when a skeletonization algorithm is applied to a network (see Fig. 2). By tracking

the original gray-scale images, we ensure that even if the branch point position determined by the skeletonization routine is slightly inaccurate, the tracked motion of the node can still be of high quality.

Using cross-correlations to find a deformation field is not new. One prominent use is in particle image velocimetry (PIV) ([**WEA13**] [**SMS16**]). Typically in this approach, feature regions are selected at regularly spaced intervals that cover the whole image stack at an initial time point and at a later time point. The features from the initial time point are then cross-correlated with a search region at a later time point to determine the relative displacement of each region. This may seem very similar to the approach we report here, but there are important differences. To successfully find the deformation field using PIV, each region must encompass a distinct feature that can be accurately located in the next time point; therefore, PIV techniques are particularly poor at tracking highly oriented structures in which the correlation function shows very broad peaks along the primary direction of alignment. Moreover, since features in PIV are defined at regularly spaced intervals, for a dilute biopolymer network these regions need to be relatively large to ensure that they contain enough fibers and branch points to be properly located. The resulting deformation field is, therefore, inherently very coarse. By instead cross-correlating regions centered around branch points as we do here, we can use a much smaller region that only encompasses a single feature itself. We can thereby track the structural deformation on a much finer level and with less computational effort. Moreover, a cross-correlation determines the relative translated movement between two images or image regions. It cannot, for instance, find rotations or deformations smaller than the region. Since the region used for PIV is large, as the fibers in the network deform by bending or buckling the cross-correlation of a region often fails. We found that in a deforming biopolymer network, the branch points typically deform much less than the surrounding fibers. Therefore, by using a small region centered around a branch point, we can still successfully track the motion of the network.

Our method was designed to track the deformation of a network as it undergoes a simple shear deformation. To track the deformation, we place our search region at the expected location of a network undergoing a simple shear deformation. This informed placement allows us to track the motion of a branch point even if its displacement is very large as long its actual position is a small displacement from its expected position. Tracking such absolutely large displacements would be difficult in other techniques such as PIV. In this paper, we assume that the network primarily deforms according to an affine shear deformation; however, we expect that this technique could be easily extended to other deformations. Moreover, if the overall network deformation does not lead to a significant amount of motion from one image stack to the next, we could center our search region around a branch point's position in the previous image stack. Thus, our approach should be applicable to a wide range of questions.

6. Material and Methods

For a complete overview of materials and methods please see [**Jaw13**].

6.1. Polymerization of fibrin networks. Fibrinogen (FIB3, Enzyme Research Labs, South Bend, IN) is diluted into buffer ($150mMNaCl$, $20mMHEPES$, and $20mMCaCl_2$ $pH7.4$). A small amount of fluorescently labelled fibrinogen (final ratio 6 : 1) is added to allow the sample to be visualized using fluorescence microscopy. Polymerization into a network is initiated by the addition of thrombin (H-T 1002a, Enzyme Research Labs, South Bend, IN) with a final concentration of $0.1U/ml$.

6.2. Application of shear and acquisition of fluorescent images. Briefly, the method can be described as follows. Two parallel glass plates with a spacing of $800\mu m$ are constructed on a fluorescent confocal microscope (Leica SP5). Quickly, after the addition of thrombin, a fibrinogen solution is pipetted between these plates. Mineral oil is added around the plates to avoid evaporation and the sample is incubated for at least six hours to allow polymerization to complete. Once polymerization is complete the network is sheared by moving the top glass plate in approximately $8\mu m$ steps leading to an approximate shear, γ, of -1%. Between each step, a set of images corresponding to the three-dimensional volume corresponding to a field-of-view of approximately $250\mu mx250\mu mx100\mu m$ is acquired. For a more complete description, please see [**Jaw13**] [**MJL13**].

6.3. Details of application of tracking algorithm. To find the skeleton, the image stack representing the undeformed network is smoothed using a $3D$ Gaussian filter (size: $5x5x5$, sigma: 0.5) and then thresholded by eye. We have used the commercial software AMIRA (FEI Software, Ver 5.3) to extract the skeleton of the network. The skeleton is saved as a text file that is imported as coordinates into MATLAB (The MathWorks, Inc.)

The algorithm we describe here was implemented using MATLAB (The MathWorks, Inc.). Fourier transforms were used for the implementation of the cross-correlations to increase processing speed.

We define the XY directions to be parallel to the imaging plane. The $-y$ direction is the direction of applied shear.

6.4. Image production for this paper. All grayscale images in this paper represent a maximum intensity projection along the x-axis of a region in three-dimensions taken from a fibrin network (Figures 5, 9, 1).

For Fig. 9, we have applied the StackReg plugin with an affine transformation using FIJI to a movie of the maximum intensity projection of a whole network as it is sheared ([**SACF12**] [**SRE12**]). The images shown in Fig. 9 are a small region from this movie that have been scaled by a factor of 3 for clarity.

7. Acknowledgements

We would like to thank Stefan Münster and Mona Rozovich for careful reading of the manuscript. We would also like to thank Björn Jawerth for useful discussions and guidance.

We acknowledge support from the National Science Foundation (DMR-1310266), the Harvard Materials Research Science and Engineering Center (DMR- 1420570).

References

[BKC08] Poul M. Bendix, Gijsje H. Koenderink, Damien Cuvelier, Zvonimir Dogic, Bernard N. Koeleman, William M. Brieher, Christine M. Field, L. Mahadevan, and David A. Weitz, *A quantitative analysis of contractility in active cytoskeletal protein networks*, Biophysical Journal **94** (2008), no. 8, 3126 – 3136.

[BM14] C. P. Broedersz and F. C. MacKintosh, *Modeling semiflexible polymer networks*, Rev. Mod. Phys. **86** (2014), 995–1036.

[BMLM11] Chase P. Broedersz, Xiaoming Mao, Tom C. Lubensky, and Frederick C. MacKintosh, *Criticality and isostaticity in fibre networks*, Nat Phys **7** (2011), no. 12, 983–988.

[Jaw13] L.M. Jawerth, *The mechanics of fibrin networks and their alterations by platelets*, Ph.D. thesis, Harvard University, 2013.

[JMV10] Louise M Jawerth, Stefan Münster, David A Vader, Ben Fabry, and David A Weitz, *A blind spot in confocal reflection microscopy: the dependence of fiber brightness on fiber orientation in imaging biopolymer networks*, Biophysical Journal **98** (2010), no. 3, L1–L3.

[KML12] Patrick Krauss, Claus Metzner, Janina Lange, Nadine Lang, and Ben Fabry, *Parameter-free binarization and skeletonization of fiber networks from confocal image stacks*, PLoS ONE **7** (2012), no. 5, 1–8.

[LMS15] Albert J Licup, Stefan Münster, Abhinav Sharma, Michael Sheinman, Louise Jawerth, Ben Fabry, David A Weitz, and Fred C. MacKintosh, *Stress controls the mechanics of collagen networks*, Proceedings of the National Academy of Sciences **112** (2015), no. 31.

[MJL13] Stefan Münster, Louise M Jawerth, Beverly A Leslie, Jeffrey I Weitz, Ben Fabry, and David A Weitz, *Strain history dependence of the nonlinear stress response of fibrin and collagen networks*, Proceedings of the National Academy of Sciences **110** (2013), no. 30, 12197–12202.

[MKJ95] MacKintosh, Käs, and Janmey, *Elasticity of semiflexible biopolymer networks.*, Phys Rev Lett **75** (1995), no. 24, 4425–4428.

[MMJ] Walter Mickel, Stefan Münster, Louise M Jawerth, David A Vader, David A Weitz, Adrian P Sheppard, Klaus Mecke, Ben Fabry, and Gerd E Schröder-Turk, *Robust pore size analysis of filamentous networks from three-dimensional confocal microscopy*, Biophysical Journal **95** (2008), no. 12, 6072–6080.

[SACF12] Johannes Schindelin, Ignacio Arganda-Carreras, Erwin Frise, Verena Kaynig, Mark Longair, Tobias Pietzsch, Stephan Preibisch, Curtis Rueden, Stephan Saalfeld, Benjamin Schmid, Jean-Yves Tinevez, Daniel James White, Volker Hartenstein, Kevin Eliceiri, Pavel Tomancak, and Albert Cardona, *Fiji: an open-source platform for biological-image analysis.*, Nat Methods **9** (2012), no. 7, 676–682.

[SMS16] Julian Steinwachs, Claus Metzner, Kai Skodzek, Nadine Lang, Ingo Thievessen, Christoph Mark, Stefan Munster, Katerina E Aifantis, and Ben Fabry, *Three-dimensional force microscopy of cells in biopolymer networks*, Nat Meth **13** (2016), no. 2, 171–176.

[SPM05] Cornelis Storm, Jennifer J. Pastore, F. C. MacKintosh, T. C. Lubensky, and Paul A. Janmey, *Nonlinear elasticity in biological gels.*, Nature **435** (2005), no. 7039, 191–194.

[SRE12] Jerry Westerweel, Gerrit E. Elsinga, and Ronald J. Adrian, *Particle image velocimetry for complex and turbulent flows*, Annual review of fluid mechanics. Volume 45, 2013, Annu. Rev. Fluid Mech., vol. 45, Annual Reviews, Palo Alto, CA, 2013, pp. 409–436, DOI 10.1146/annurev-fluid-120710-101204. MR3026125

[SVJ08] Andrew M. Stein, David A. Vader, Louise M. Jawerth, David A. Weitz, and Leonard M. Sander, *An algorithm for extracting the network geometry of three-dimensional collagen gels*, J. Microsc. **232** (2008), no. 3, 463–475, DOI 10.1111/j.1365-2818.2008.02141.x. MR2649407

[WEA13] Jerry Westerweel, Gerrit E. Elsinga, and Ronald J. Adrian, *Particle image velocimetry for complex and turbulent flows*, Annu. Rev. Fluid Mech., vol. 45, 2013, pp. 409–436, DOI 10.1146/annurev-fluid-120710-101204. MR3026125

[XVH] Ting Xu, Dimitrios Vavylonis, and Xiaolei Huang, *3d actin network centerline extraction with multiple active contours*, Medical Image Analysis **18**, no. 2, 272–284.

Department of Physics, Harvard University, Cambridge, Massachusetts 02138
Current address: Max Planck for the Physics of Complex Systems, 01187 Dresden Germany
E-mail address: ljawerth@post.harvard.edu

Department of Physics and the School of Engineering and Applied Sciences, Harvard University, Cambridge, Massachusetts 02138
E-mail address: weitz@seas.harvard.edu